ЖУРНАЛ ФІЗИЧНИХ ДОСЛІДЖЕНЬ
т. 13, № 4 (2009) 4001(7 с.)

JOURNAL OF PHYSICAL STUDIES
v. 13, No. 4 (2009) 4001(7 p.)

CATALYTIC CO OXIDATION REACTION: LATTICE MODELS AND KINETIC DESCRIPTION

I. S. Bzovska, I. M. Mryglod
Institute for Condensed Matter Physics of the National Academy of Sciences of Ukraine, 1, Svientsitskii St., Lviv, UA–79011, Ukraine
(Received October 16, 2009)

The kinetics of processes of the catalytic CO oxidation is studied. On the basis of a kinetic model the stationary points of the system are found and the analysis of their stability is performed. It is revealed that at intermediate values of CO pressures the system has two stable points, so it is in the bistable state. In the framework of the lattice-gas model the effect of inactive adsorbed impurities on the kinetics of the reaction is investigated. It is shown that for slow impurities the bistable region is more narrow in comparison with the case of their fast dynamics when the distribution of impurities on the surface can be assumed equilibrium. Phase diagrams are investigated at the temperature $T = 0$ by incorporating the nearest-neighbor interactions on a catalyst surface. The conditions of the existence of nonuniform phases depending on the interaction parameters are established.

Key words: lattice-gas model, catalysis, oxidation, carbon monoxide, oxygen, phase diagrams.

PACS number(s): 05.50.+q, 68.43.−h, 82.65.+r

I. INTRODUCTION

CO oxidation on Pt-group metals has been attracting the attention of chemists, physicists, and mathematicians due to richness of its spatiotemporal kinetics exhibiting bistability, oscillations, chaos, and pattern formation [1–8]. This reaction is also of interest from the point of view of applied chemical engineering because it plays an important role in the treatment of automotive exhaust gases.

The basic steps of the reaction are the adsorption of the reacting species on the surface, their reaction and the desorption of the product (the Langmuir–Hinshelwood process) [9]. The adsorption of the catalyst causes a change in the state of the reactant, possibly including disassociation, which allows the reaction to take place. The final desorption step is necessary for the product to be recovered and for the catalyst to be regenerated. With realistic values of the corresponding rate constants, these steps alone allow one often (especially under the UHV conditions) to explain the reaction bistability [10, 11].

In our paper we will use the classical approach for the kinetics of these processes and consider average concentrations of the adsorbed species. Section II contains the kinetic description of the CO catalytic oxidation reaction and its general properties. In section III the effect of adsorbed impurities on the reaction is investigated in the framework of the lattice-gas model. Section IV presents phase diagrams at the temperature $T = 0$ by incorporating the nearest-neighbor interactions on a catalyst surface. Finally, in section V we present our conclusions.

II. KINETIC DESCRIPTION OF THE CO CATALYTIC OXIDATION REACTION

The equations of reactions that can proceed in the course of carbon monoxide oxidation on the catalyst surface look like

$$\mathrm{O_2} + 2* \rightarrow 2\mathrm{O^{ads}}, \tag{1}$$

$$\mathrm{CO} + * \rightleftharpoons \mathrm{CO^{ads}}, \tag{2}$$

$$\mathrm{CO^{ads}} + \mathrm{O^{ads}} \rightarrow \mathrm{CO_2} + 2*, \tag{3}$$

where the asterisk denotes a free active site on the catalyst surface. Oxygen desorption is not considered because it is usually almost impossible at the temperature conditions of most experiments [12].

Let us consider a model that represents an ideal adsorbate layer model where the interactions between adsorbed molecules are neglected. So the evolution of the CO and oxygen coverages in time on the catalyst surface are determined by the set of kinetic equations

$$\frac{\mathrm{d}\theta_{\mathrm{CO}}}{\mathrm{dt}} = p_{\mathrm{CO}} k_{\mathrm{CO}} s_{\mathrm{CO}} (1 - \theta_{\mathrm{CO}} - \theta_{\mathrm{O}}) - d\theta_{\mathrm{CO}} - k\theta_{\mathrm{CO}}\theta_{\mathrm{O}}, \tag{4}$$

$$\frac{\mathrm{d}\theta_{\mathrm{O}}}{\mathrm{dt}} = 2p_{\mathrm{O_2}} k_{\mathrm{O}} s_{\mathrm{O}} (1 - \theta_{\mathrm{CO}} - \theta_{\mathrm{O}})^2 - k\theta_{\mathrm{CO}}\theta_{\mathrm{O}}, \tag{5}$$

where $d = d_0 \exp(-\beta E_d)$ denotes the rate of CO desorption, p_{CO} and $p_{\mathrm{O_2}}$ are partial pressures of CO and oxygen respectively, k_{CO} and k_{O} are the CO and oxygen impingement rates, s_{CO} and s_{O} are the corresponding sticking coefficients. The coefficient k denotes the reaction rate constant and is given by $k = k_{\mathrm{CO_2}} \exp(-\beta E_0)$, where E_0 is the activation energy of the reaction. The first equation, Eq. (4), describes variations in the amount of the adsorbed CO, a chemical reaction with the adsorbed oxygen, and desorption of CO with the desorption constant d. The first term in Eq. (5) describes the dissociative adsorption of oxygen, and the second one refers to the reaction between adsorbed oxygen and CO.

In general the model as described by Eqs. (4), (5) can exhibit four stationary points. One is given by

$$\theta^s_{\mathrm{CO}} = 0, \quad \theta^s_{\mathrm{O}} = 1, \tag{6}$$

which corresponds to the oxygen poisoning on the substrate. It should be noted that this solution is never observed experimentally. The others are given by the roots of cubic equation for $\theta_{\rm CO}$,

$$A(\theta^s_{\rm CO})^3 + B(\theta^s_{\rm CO})^2 + C\theta^s_{\rm CO} + D = 0, \tag{7}$$

and the corresponding oxygen concentration is given by

$$\theta^s_{\rm O} = \frac{p_{\rm CO}k_{\rm CO}s_{\rm CO}(1-\theta^s_{\rm CO})}{p_{\rm CO}k_{\rm CO}s_{\rm CO}+k\theta^s_{\rm CO}} - \frac{d\theta^s_{\rm CO}}{p_{\rm CO}k_{\rm CO}s_{\rm CO}+k\theta^s_{\rm CO}}. \tag{8}$$

The coefficients of the cubic equation are

$$\begin{aligned} A &= 2p_{\rm O_2}k_{\rm O}s_{\rm O}k^2,\\ B &= -4p_{\rm O_2}k_{\rm O}s_{\rm O}k(k+d) + k^2(p_{\rm CO}k_{\rm CO}s_{\rm CO}+d),\\ C &= 2p_{\rm O_2}k_{\rm O}s_{\rm O}k(k+2d) + 2p_{\rm O_2}k_{\rm O}s_{\rm O}d^2\\ &\quad + kp_{\rm CO}k_{\rm CO}s_{\rm CO}(p_{\rm CO}k_{\rm CO}s_{\rm CO}+d-k),\\ D &= -p^2_{\rm CO}k^2_{\rm CO}s^2_{\rm CO}k. \end{aligned} \tag{9}$$

In general, for the numerical values of the adsorption constants, there is only one positive real root to this equation, the two others being imaginary. All the roots can be real if the following condition

$$\left(\frac{C}{3A} - \left(\frac{B}{3A}\right)^2\right)^3 + \left(\left(\frac{B}{3A}\right)^3 - \frac{BC}{6A^2} + \frac{D}{2A}\right)^2 < 0 \tag{10}$$

is satisfied. From the physical point of view, when all the roots of the cubic equation are real we shall have the bistable region at the phase diagrams. So inequality (10) gives in fact the condition of the existence of the bifurcation region that follows from the kinetic level of description.

We now characterize the stationary points by their eigenvalues in the time evolution of Eqs. (4), (5). This analysis reveals the stability of the stationary points. For this, we introduce small perturbations around the stationary solutions and write $\theta_{\rm CO}$ and $\theta_{\rm O}$ as

$$\theta_{\rm CO} = \theta^s_{\rm CO} + \delta\theta_{\rm CO}(t), \quad \theta_{\rm O} = \theta^s_{\rm O} + \delta\theta_{\rm O}(t), \tag{11}$$

where $\theta^s_{\rm CO}$ and $\theta^s_{\rm O}$ are the coordinates of a stationary point and $\delta\theta_{\rm CO}$ and $\delta\theta_{\rm O}$ are small time-dependent perturbations. The linearized equations are then

$$\frac{\rm d}{{\rm d}t}\begin{pmatrix}\delta\theta_{\rm O}\\ \delta\theta_{\rm CO}\end{pmatrix} = \begin{pmatrix}-4h_{\rm O}v^s - k\theta^s_{\rm CO} & -4h_{\rm O}v^s - k\theta^s_{\rm O}\\ -h_{\rm CO} - k\theta^s_{\rm CO} & -h_{\rm CO} - d - k\theta^s_{\rm O}\end{pmatrix} \times \begin{pmatrix}\delta\theta_{\rm O}\\ \delta\theta_{\rm CO}\end{pmatrix} \tag{12}$$

with $v^s = 1 - \theta^s_{\rm O} - \theta^s_{\rm CO}$ being the stationary density of empty adsorption sites. The following notations $h_{\rm O} = p_{\rm O_2}k_{\rm O}s_{\rm O}$, $h_{\rm CO} = p_{\rm CO}k_{\rm CO}s_{\rm CO}$ are introduced for the convenience. The determination of the eigenvalues of the matrix in Eq. (12) allows us to analyze the type of stability of the stationary solutions found above.

From the condition of the existence of the bifurcation region (10) for the model parameters $p_{\rm O_2} = 1.5\cdot10^{-5}$ Torr, $k_{\rm O} = 7.8\cdot10^5{\rm s}^{-1}\,{\rm Torr}^{-1}$, $k_{\rm CO} = 7\cdot10^6{\rm s}^{-1}\,{\rm Torr}^{-1}$, $k = 598{\rm s}^{-1}$, $d = 0.27{\rm s}^{-1}$, $s_{\rm CO} = 0.9$, $s_{\rm O} = 0.06$, which corresponded to the Pt(111) surface [13], the bistable region exists at the following values of pressure $p_{\rm CO}$:

$$p^{\rm (min)}_{\rm CO} < p_{\rm CO} < p^{\rm (max)}_{\rm CO} \tag{13}$$

with $p^{\rm (min)}_{\rm CO} = 1.53\cdot10^{-7}\,{\rm Torr}$ and $p^{\rm (max)}_{\rm CO} = 2.05\cdot10^{-7}\,{\rm Torr}$. Let us consider these three cases of low ($p_{\rm CO} < p^{\rm (min)}_{\rm CO}$), intermediate ($p^{\rm (min)}_{\rm CO} < p_{\rm CO} < p^{\rm (max)}_{\rm CO}$) and high ($p_{\rm CO} > p^{\rm (max)}_{\rm CO}$) values of partial pressures $p_{\rm CO}$. The stationary points, their eigenvalues and the corresponding types of their stability are shown in Table. Phase portraits and typical trajectories of the model in the $(\theta_{\rm CO}, \theta_{\rm O})$ parameter space for all cases are shown in Figs. 1–2.

Pressure $p_{\rm CO}$	Stationary points	Eigenvalues	Stability
10^{-7} Torr	$(\theta_{\rm CO}=0,\,\theta_{\rm O}=1)$	0.63 −599.5	saddle
	$(\theta_{\rm CO}=0.0009,\,\theta_{\rm O}=0.55)$	−0.63 −331	stable node
$1.68\cdot10^{-7}$ Torr	$(\theta_{\rm CO}=0,\,\theta_{\rm O}=1)$	1.05 −600.38	saddle
	$(\theta_{\rm CO}=0.005,\,\theta_{\rm O}=0.24)$	−1.00 −150.48	stable node
	$(\theta_{\rm CO}=0.35,\,\theta_{\rm O}=0.003)$	0.48 −211.68	saddle
	$(\theta_{\rm CO}=0.7,\,\theta_{\rm O}=0.0003)$	−0.50 −422.98	stable node
$2.2\cdot10^{-7}$ Torr	$(\theta_{\rm CO}=0,\,\theta_{\rm O}=1)$	1.38 −601	saddle
	$(\theta_{\rm CO}=0.8,\,\theta_{\rm O}=0.00001)$	−1.09 −479.58	stable node

Table 1. Analysis of the stability of the stationary points at different values of pressure $p_{\rm CO}$.

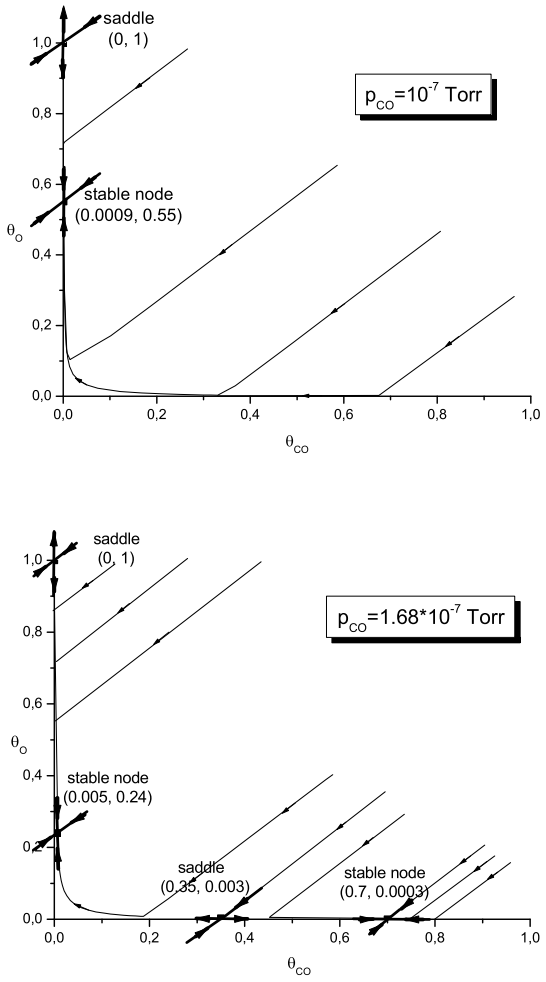

Fig. 1. Phase portraits and typical trajectories of the model in the $(\theta_{\rm CO}, \theta_{\rm O})$ parameter space at $p_{\rm CO} = 10^{-7}$ Torr and $p_{\rm CO} = 1.68 \cdot 10^{-7}$ Torr.

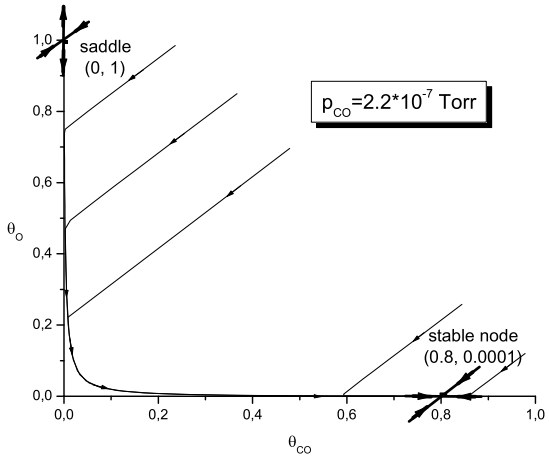

Fig. 2. Phase portrait and typical trajectories of the model in the $(\theta_{\rm CO}, \theta_{\rm O})$ parameter space at $p_{\rm CO} = 2.2 \cdot 10^{-7}$ Torr.

As is seen from Fig. 1, in the case of low pressure $p_{\rm CO}$ ($p_{\rm CO} = 10^{-7}$ Torr) the system has only one stable point ($\theta_{\rm CO} = 0.0009$, $\theta_{\rm O} = 0.55$), which corresponds to oxygen adsorption on the surface of the catalyst. This is a reactive region in the bifurcation diagram. At the pressure $p_{\rm CO} = 1.68 \cdot 10^{-7}$ Torr the system has two stable nodes ($\theta_{\rm CO} = 0.005$, $\theta_{\rm O} = 0.24$) and ($\theta_{\rm CO} = 0.7$, $\theta_{\rm O} = 0.0003$). So the system can exhibit the properties of a bistable state with jumps from one stable branch onto the other. As is shown in Fig. 2, at $p_{\rm CO} = 2.2 \cdot 10^{-7}$ Torr the system similarly to the case of low pressure $p_{\rm CO}$ has only one stable point, but the situation is changed because the stable state is now characterized by a high CO coverage on surface and practically absent oxygen ($\theta_{\rm CO} = 0.8$, $\theta_{\rm O} = 0.0001$). This corresponds to an inactive region in the bifurcation diagram. Note also a huge difference in the eigenvalues (see Table) found for all stationary solutions (two orders of magnitude). This, in particular, explain already the existence of two different time relaxation scales for the model considered.

Phase diagram in the $(p_{\rm CO}, 1/T)$ parameter space depicted in Fig. 3 reveals a bistability region. The lower and upper branches of the bifurcation are calculated from Eq. (10).

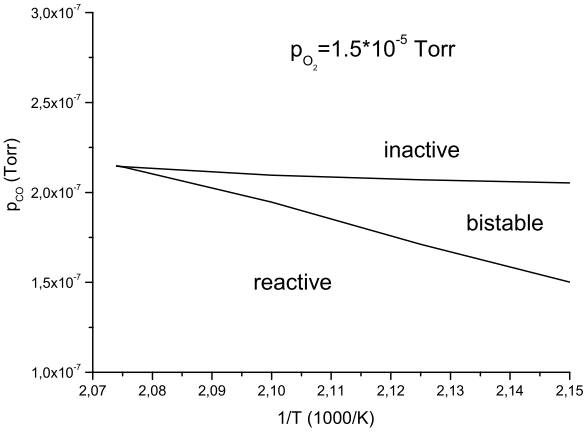

Fig. 3. Phase diagram $(p_{\rm CO}, 1/T)$ of the model at oxygen partial pressure $p_{\rm O_2} = 1.5 \cdot 10^{-5}$ Torr.

Summarizing, we may say that at low $p_{\rm CO}$ the surface of the catalyst is predominantly covered by adsorbed oxygen. Increasing pressure $p_{\rm CO}$ causes the oxygen coverage to decrease and at a certain value of $p^c_{\rm CO} = 1.683 \cdot 10^{-7}$ Torr it follows sharply to zero whereas carbon monoxide coverage at the moment is suddenly increased. First-order phase transition at $p_{\rm CO} = p^c_{\rm CO}$ from a reactive state with medium O coverage to an inactive state where the surface is predominantly covered by CO occurs.

III. THE EFFECT OF ADSORBED IMPURITIES ON THE REACTION

Let us consider how the presence of passive impurities on a catalyst's surface affects the kinetics of the reaction studied in the previous section. For this we will use

a lattice-gas reaction model. So the Hamiltonian of the system is

$$H = -\mu_1 \sum_i n_i^1 - \mu_2 \sum_i n_i^2 - \mu_3 \sum_i n_i^3 + w_1 \sum_{\langle ij \rangle} n_i^1 n_j^1 + w_2 \sum_{\langle ij \rangle} n_i^2 n_j^2 + \varepsilon_{12} \sum_{\langle ij \rangle} n_i^1 n_j^2 + \varepsilon_{13} \sum_{\langle ij \rangle} n_i^1 n_j^3 + \varepsilon_{23} \sum_{\langle ij \rangle} n_i^2 n_j^3, \tag{14}$$

where μ_1, μ_2 and μ_3 denote the chemical potentials of CO, O and impurity respectively, and w_1, w_2, ε_{12}, ε_{13} and ε_{23} are the interaction energies between the nearest-neighbor CO–CO, O–O, CO–O, CO-impurity and O-impurity, respectively. The following notations for three types of adsorbate occupancies of the ith surface site are: n_i^1 for an adsorbed CO molecule, n_i^2 for adsorbed oxygen and n_i^3 for adsorbed impurity, $n_i^l = [0, 1]$ and l=1,2,3. The condition $n_i^1 + n_i^2 + n_i^3 \leq 1$ precludes the adsorbed particles from occupying the same adsorption site. $\sum_{\langle ij \rangle}$ means the sum over the nearest-neighbor pairs.

The Hamiltonian of the system in the mean-field approximation looks like

$$H = -\widetilde{\mu}_1 \sum_i n_i^1 - \widetilde{\mu}_2 \sum_i n_i^2 - \widetilde{\mu}_3 \sum_i n_i^3 + AN, \tag{15}$$

where the following notations are introduced:

$$\begin{aligned} A &= -w_1 \langle n^1 \rangle^2 - w_2 \langle n^2 \rangle^2 - \varepsilon_{12} \langle n^1 \rangle \langle n^2 \rangle - \varepsilon_{13} \langle n^1 \rangle \langle n^3 \rangle - \varepsilon_{23} \langle n^2 \rangle \langle n^3 \rangle, \\ \widetilde{\mu}_1 &= \mu_1 - 2w_1 \langle n^1 \rangle - \varepsilon_{12} \langle n^2 \rangle - \varepsilon_{13} \langle n^3 \rangle, \\ \widetilde{\mu}_2 &= \mu_2 - 2w_2 \langle n^2 \rangle - \varepsilon_{12} \langle n^1 \rangle - \varepsilon_{23} \langle n^3 \rangle, \\ \widetilde{\mu}_3 &= \mu_3 - \varepsilon_{13} \langle n^1 \rangle - \varepsilon_{23} \langle n^2 \rangle, \end{aligned} \tag{16}$$

$\widetilde{\mu}_i$ are the so-called modified chemical potentials. Using the thermodynamic formula $\theta_i = -\dfrac{1}{N} \left(\dfrac{\partial \Omega}{\partial \mu_i} \right)_T$ where Ω is the grand thermodynamic potential we obtain the following system of equations for the coverages θ_i:

$$\theta_i = \frac{\exp\left(\dfrac{\widetilde{\mu}_i}{kT}\right)}{1 + \sum\limits_{i=1}^{3} \exp\left(\dfrac{\widetilde{\mu}_i}{kT}\right)}, \qquad i = 1, 2, 3. \tag{17}$$

In the case when the reaction rate is higher than the rates of adsorbate adsorption and desorption, the evolutions of the CO and O coverages in time are determined by the kinetic equations

$$\frac{\mathrm{d}\theta_1}{\mathrm{d}t} = p_{\mathrm{CO}} k_{\mathrm{CO}} s_{\mathrm{CO}} (1 - \theta_1 - \theta_2 - \theta_3) - d\theta_1 - k\theta_1\theta_2, \tag{18}$$

$$\frac{\mathrm{d}\theta_2}{\mathrm{d}t} = 2p_{\mathrm{O}_2} k_{\mathrm{O}} s_{\mathrm{O}} (1 - \theta_1 - \theta_2 - \theta_3)^2 - k\theta_1\theta_2. \tag{19}$$

Then, in order to analyze the stable states, it is necessary to solve the equations $\mathrm{d}\theta_1/\mathrm{d}t = 0$ and $\mathrm{d}\theta_2/\mathrm{d}t = 0$ together with equations (17) with respect to the average coverages for CO and oxygen.

In the case of equilibrium impurities with slow self dynamics, compared with the reaction rate, the impurities distribution on the surface cannot be assumed to be equilibrium. So the kinetic equation for such impurities can be written as

$$\frac{\mathrm{d}\theta_3}{\mathrm{d}t} = k_a (1 - \theta_1 - \theta_2 - \theta_3) - k_d \theta_3, \tag{20}$$

where the coefficients k_a and k_d are the rates of adsorption and desorption of the impurities. Again, to analyze the stable states of the system, it is necessary to solve the equation $\mathrm{d}\theta_3/\mathrm{d}t = 0$ together with equations (17)-(19) with respect to the average coverages for CO and oxygen.

In Figure 4 the dependencies of the average CO and oxygen coverages as the functions of p_{CO} are shown for three different cases — for a pure surface without any impurities, for the surface with impurities when their concentration θ_d on the surface is constant, $\theta_d = 0.1$, and for the surface with impurities, concentration of which is determined by the kinetic equation (20).

We can see from the figure that the presence of the impurities narrows the bistable region and shifts it to the region of lower pressures p_{CO}, but in the case of impurities with slow self dynamics the bistable region is narrowed far more than in the case when their dynamics is fast.

From kinetic equations (18)–(20) we can estimate a width of the bistable region in the presence of slow impurities. For the model parameters, which are correspondent to the Pt(111) surface, the bistable region exists at the following values of pressure p_{CO}:

$$1.42 \cdot 10^{-7} \quad \text{Torr} < p_{\mathrm{CO}} < 1.67 \cdot 10^{-7} \quad \text{Torr}. \tag{21}$$

The coefficients $k_a = 0.05\text{c}^{-1}$, $k_d = 0.2\text{c}^{-1}$ are chosen in such a way so as to obtain small impurities concentrations on the surface. For comparison, the results of calculations for the bistability bounds for the model without impurities are $p_{\text{CO}}^{\min} = 1.53 \times 10^{-7}$ Torr and $p_{\text{CO}}^{max} = 2.05 \times 10^{-7}$ Torr. As we see, the width of the bistability region has a tendency to its narrowing as a result of the presence of impurities.

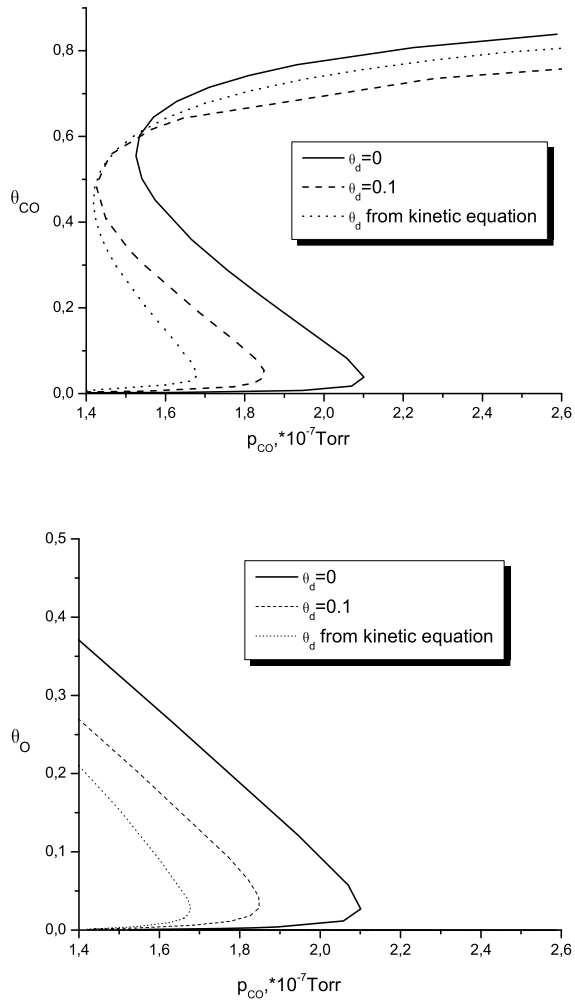

Fig. 4. Average CO and oxygen coverages as the functions of p_{CO} at $T = 466\,\text{K}$ and for various values of the concentrations θ_d.

IV. GROUND-STATE DIAGRAMS FOR LATTICE-GAS MODEL OF CATALYTIC CO OXIDATION

To reveal what states are realized on a pure surface at low temperatures let us consider lattice-gas model at zero temperature. We will follow in our study the method proposed in Ref. [14]. The idea of the method is as follows. If the Hamiltonian of the system can be rewritten in the form of the sum over the nearest-neighbor bonds on a lattice then the region on the phase diagram which corresponds to such particular bond is determined from the condition of the minimum of the energy of this bond. We will consider two-dimensional square lattice with the same number of bonds around each site. So the Hamiltonian of the model written in the form of the sum over the nearest-neighbor bonds on a lattice is as follows:

$$H = -\frac{\mu_1}{4}\sum_{\langle ij\rangle}(n_i^1 + n_j^1) - \frac{\mu_2}{4}\sum_{\langle ij\rangle}(n_i^2 + n_j^2) + w_1\sum_{\langle ij\rangle} n_i^1 n_j^1 + w_2\sum_{\langle ij\rangle} n_i^2 n_j^2 + \varepsilon_{12}\sum_{\langle ij\rangle} n_i^1 n_j^2. \quad (22)$$

We will construct the ground-state diagrams in the (μ_1, μ_2) plane. Each region on this plane corresponding to a separate two-site block is determined by the system of inequalities obtained from the condition of the minimum of the block energy. The uniform regions *–*, CO–CO and O–O exist always, the region CO–O, where the reaction of catalytic CO oxidation takes place exists on condition that $\varepsilon_{12} < \frac{1}{2}(w_1 + w_2)$. The nonuniform regions *–CO, *–O exist on conditions that $w_1 > 0$, $w_2 > 0$, respectively. The increase of the interaction parameters w_1 and w_2 leads to the corresponding extension of the regions *–CO, *–O. And vice versa, the region CO-O is extended with the decrease of the parameter ε_{12}. If $\varepsilon_{12} > \frac{1}{2}(w_1 + w_2)$, $w_1 < 0$, $w_2 < 0$, there are no nonuniform phases at all.

The ground-state diagrams of the model are shown in Figures 5 and 6. The coordinates of intersection points on the diagrams can be calculated analytically. As an example, we represent them for the poorest (Fig. 5(a)) and for one of the richest (Fig. 6(a)) diagrams. For the first diagram the coordinates of the intersection point are $(w_1/2, w_2/2)$. The second diagram where all the nonuniform regions exist has four intersection points with the following coordinates: point I — (ε_{12}, w_2), II — $(\varepsilon_{12}, \varepsilon_{12})$, III — (w_1, ε_{12}) and IV — (0, 0). The coordinates of intersection points for other diagrams can be also found easily.

The diagrams are symmetric with respect to the bisectrix of the angle $\mu_2 O \mu_1$. Actually, replacing the axes μ_1 and μ_2 as well as the notations CO and O we will obtain the same diagrams. That is why we present here only diagrams for CO.

As one can see, twelve topologically nonequivalent diagrams are obtained (including three diagrams for oxygen not presented here): eight types of diagrams for $\varepsilon_{12} < \frac{1}{2}(w_1 + w_2)$ where the region CO – O exists and four diagrams for $\varepsilon_{12} > \frac{1}{2}(w_1 + w_2)$ without this region. We note that model (22) is isomorphous to a spin–1 Ising model.

To incorporate the effect of passive impurities on a surface we must add several terms to Hamiltonian (22):

$$H = -\frac{\mu_1}{4}\sum_{\langle ij\rangle}(n_i^1 + n_j^1) - \frac{\mu_2}{4}\sum_{\langle ij\rangle}(n_i^2 + n_j^2) + w_1\sum_{\langle ij\rangle} n_i^1 n_j^1 + w_2\sum_{\langle ij\rangle} n_i^2 n_j^2 + \varepsilon_{12}\sum_{\langle ij\rangle} n_i^1 n_j^2 + \varepsilon_{13}\sum_{\langle ij\rangle} n_i^1 n_j^3 + \varepsilon_{23}\sum_{\langle ij\rangle} n_i^2 n_j^3. \quad (23)$$

We suppose that the average coverage of impurities $\langle n^3 \rangle \ll 1$ that is why the interactions between nearest-neighbor impurity — impurity can be neglected. It should be noted that obvious separation of impurities in Hamiltonian (23) ($n^3 \to c$, where c denotes impurity concentration) converts model (23) into model (22) with the renormalized parameters, namely $\mu_1 \to \mu_1 - \varepsilon^*_{13} zc$ and $\mu_2 \to \mu_2 - \varepsilon^*_{23} zc$. At the temperature $T = 0$ the entropy makes zero contribution to the thermodynamic potential and there are only contributions from the average energy and the number of particles. Consequently, in this approximation a shift of the phases along the axes $0\mu_1$, $0\mu_2$ can be observed in the phase diagrams obtained for model (22). The direction of such a shift depends on the sign of interaction parameters ε_{13} and ε_{23}, describing the coupling of CO and O with impurities, respectively.

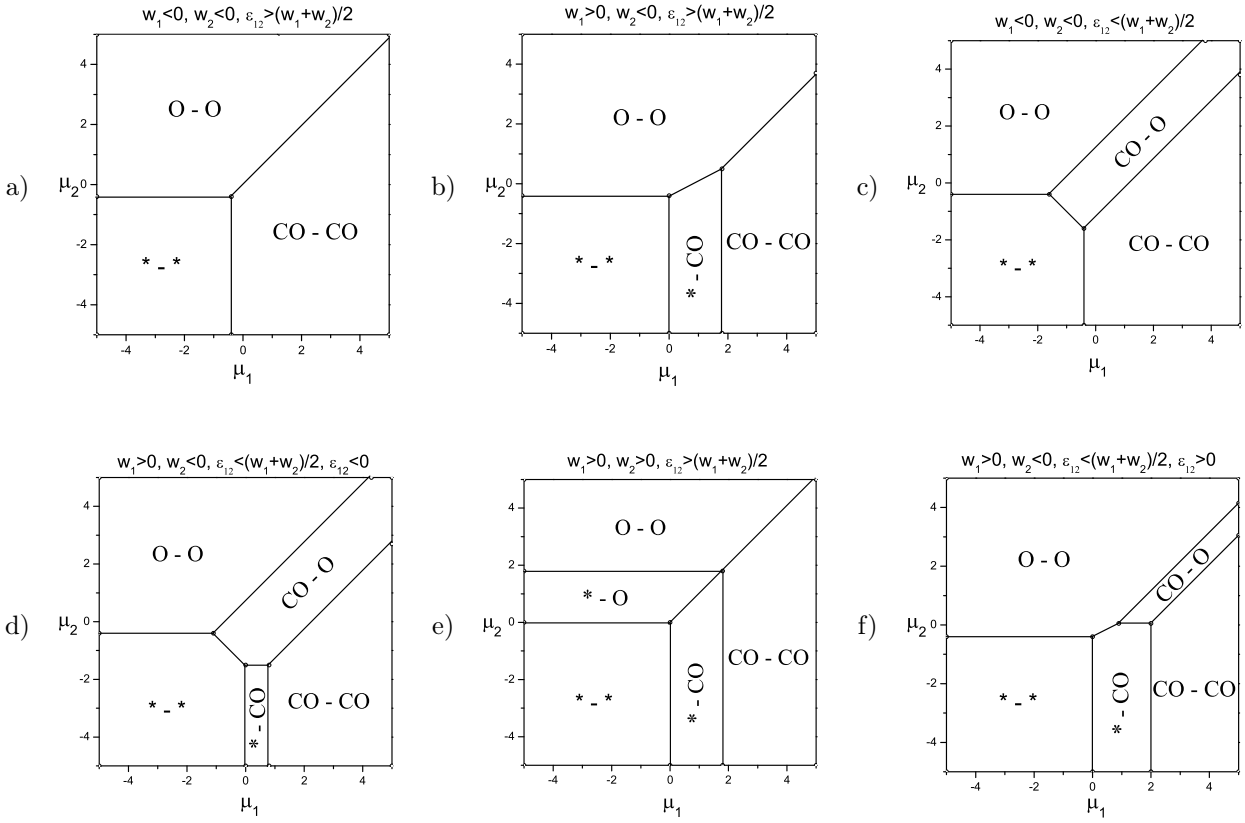

Fig. 5. Main topologies of ground-state diagrams for the model. The parameters are given in kcal/mol. (a) $w_1 = -0.8$, $w_2 = -0.8$, $\varepsilon_{12} = 1.5$; (b) $w_1 = 1.8$, $w_2 = -0.8$, $\varepsilon_{12} = 1.5$; (c) $w_1 = -0.8$, $w_2 = -0.8$, $\varepsilon_{12} = -2$; (d) $w_1 = 0.8$, $w_2 = -0.8$, $\varepsilon_{12} = -1.5$; (e) $w_1 = 1.8$, $w_2 = 1.8$, $\varepsilon_{12} = 2.5$; (f) $w_1 = 2$, $w_2 = -0.8$, $\varepsilon_{12} = 0.05$.

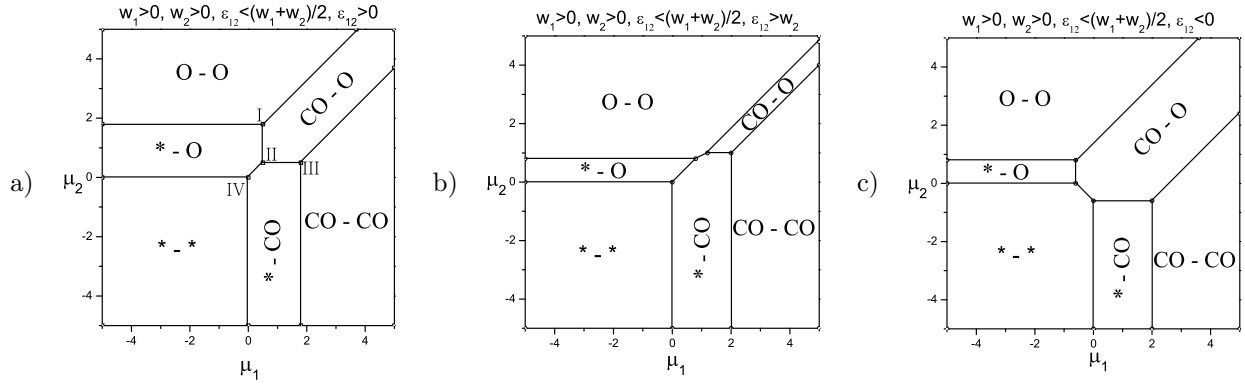

Fig. 6. Topologies of ground-state diagrams for the model in the case $w_1 > 0$, $w_2 > 0$, $\varepsilon_{12} < \frac{1}{2}(w_1 + w_2)$. The parameters are given in kcal/mol. (a) $w_1 = 1.8$, $w_2 = 1.8$, $\varepsilon_{12} = 0.5$; (b) $w_1 = 2$, $w_2 = 0.8$, $\varepsilon_{12} = -0.6$; (c) $w_1 = 2$, $w_2 = 0.8$, $\varepsilon_{12} = 1$.

V. CONCLUSIONS AND FINAL REMARKS

We have investigated a kinetic model for the catalytic CO oxidation on the surface of Pt(111). We have found the stationary points of the system and analyzed them by their eigenvalues to reveal their stability. Three different cases of low, intermediate and high pressures $p_{\rm CO}$ have been considered. As it was found, at the intermediate pressures two stable states exist and the system exhibits jumps from one stable branch onto the other. This is the bistability phenomenon. The condition of the existence of the bistable region for the model has been analytically found and the bifurcation diagram has been constructed. For the model parameters which corresponded to the Pt(111) surface the bistable region exists at CO pressures: $1.53 \cdot 10^{-7}\,\text{Torr} < p_{\rm CO} < 2.05 \cdot 10^{-7}\,\text{Torr}$.

We have investigated the effect of impurities on the kinetics of the reaction in the framework of the lattice-gas model. In the case of slow impurities the bistable region is narrowed far more than in the case when their dynamics is fast and their distribution on the surface can be assumed to be equilibrium.

Using the method developed in Ref. [14] we have constructed the ground-state diagrams for the lattice model of the reaction taking place on a surface without any impurities by incorporating nearest-neighbor interactions between co-adsorbates. We have found the conditions of existence of nonuniform phases depending on the interaction parameters. The nonuniform region CO–O where the reaction of catalytic CO oxidation takes place exists at the condition $\varepsilon_{12} < \frac{1}{2}(w_1 + w_2)$. The width of this region increases when the interaction parameter ε_{12} decreases.

[1] V. P. Zhdanov, J. Chem. Phys. **126**, 074706 (2007).
[2] P. P. Kostrobii, M. V. Tokarchuk, V. I. Alekseyev, Phys. Chem. Solid State **7**, 25 (2006).
[3] V. P. Zhdanov, Surf. Sci. **500**, 966 (2002).
[4] F. Chavez, L. Vicente, A. Perera, M. Moreau, J. Chem. Phys. **109**, 8617 (1998).
[5] Yu. Suchorski, J. Beben, R. Imbihl, E. W. James, Da-Jiang Lin, J. W. Evans, Phys. Rev. B **63**, 165417 (2001).
[6] B. C. S. Grandi, W. Figueiredo, Phys. Rev. E **65**, 036135 (2002).
[7] O. Nekhamkina, R. Digilov, M. Sheintuch, J. Chem. Phys. **119**, 2322 (2003).
[8] Y. Cisternas, Ph. Holmes, I. G. Kevrekidis, X. Li, J. Chem. Phys. **118**, 3312 (2003).
[9] R. M. Ziff, E. Gulari, Y. Barshad, Phys. Rev. Lett. **56**, 2553 (1986).
[10] V. P. Zhdanov, B. Kasemo, Surf. Sci. Rep. **20**, 111 (1994).
[11] I. M. Mryglod, I. S. Bzovska, Ukr. J. Phys. **52**, 466 (2007).
[12] R. Imbihl, G. Ertl, Chem. Rev. **95**, 697 (1995).
[13] N. Pavlenko, P. P. Kostrobij, Yu. Suchorski, R. Imbihl, Surf. Sci. **489**, 29 (2001).
[14] Yu. I. Dublenych, Phys. Rev. B **71**, 012411 (2005).

КАТАЛІТИЧНА РЕАКЦІЯ ОКИСЛЕННЯ CO: ҐРАТКОВІ МОДЕЛІ ТА КІНЕТИЧНИЙ ОПИС

І. С. Бзовська, І. М. Мриглод

Інститут фізики конденсованих систем НАН України, вул. Свєнціцького, 1, Львів, 79011, Україна

Досліджено кінетику процесів каталітичної реакції окислення монооксиду вуглецю. У межах кінетичної моделі знайдено стаціонарні точки системи та проаналізовано їх на стабільність за їхніми власними значеннями в часовій еволюції рівнянь хімічної кінетики. Виявлено, що при проміжних значеннях тисків CO система має дві стійкі точки, тобто вона перебуває в бістабільному стані. Вплив неактивних домішок на кінетику реакції досліджено на основі ґраткової моделі. Коли концентрація домішки змінюється на поверхні досить повільно, область бістабільності звужується значно більше, ніж коли динаміка домішки швидка, а її розподіл на поверхні можна вважати рівноважним. Отримано фазові діаграми при температурі $T = 0$ із урахуванням взаємодій на поверхні між найближчими сусідами. Знайдено умови існування неоднорідних областей залежно від значень параметрів взаємодії.